Adv Comput Math
DOI 10.1007/s10444-014-9390-z

Energy-conserving methods for Hamiltonian boundary value problems and applications in astrodynamics

Pierluigi Amodio · Luigi Brugnano · Felice Iavernaro

Received: 11 September 2013 / Accepted: 20 October 2014

Abstract We introduce new methods for the numerical solution of general Hamiltonian boundary value problems. The main feature of the new formulae is to produce numerical solutions along which the energy is precisely conserved, as is the case with the analytical solution. We apply the methods to locate periodic orbits in the circular restricted three body problem by using their energy value rather than their period as input data. We also use the methods for solving optimal transfer problems in astrodynamics.

Keywords Energy conserving Runge–Kutta methods · Hamiltonian boundary value problems · Astrodynamics · Optimal control

Mathematics Subject Classification (2010) 65P10 · 65L10 · 65L06

Communicated by: M. Stynes

P. Amodio · F. Iavernaro (✉)
Dipartimento di Matematica, Università di Bari, Bari, Italy
e-mail: felice.iavernaro@uniba.it

P. Amodio
e-mail: pierluigi.amodio@uniba.it

L. Brugnano
Dipartimento di Matematica e Informatica "U. Dini", Università di Firenze, Firenze, Italy
e-mail: luigi.brugnano@unifi.it

Published online: 14 November 2014

1 Introduction

We are concerned with the numerical solution of the general autonomous Hamiltonian boundary value problem

$$\begin{cases} \dot{y}(t) = J\nabla H(y(t)), & t \in [t_0, t_f], \\ g(y(t_0), y(t_f)) = 0. \end{cases} \tag{1}$$

The scalar function $H : \Omega \subset \mathbb{R}^{2m} \to \mathbb{R}$ is the *Hamiltonian* of the problem, $J = \begin{pmatrix} 0 & I_m \\ -I_m & 0 \end{pmatrix}$ (here and in the sequel I_r will denote the identity matrix of dimension r), and the vector function $g : \mathbb{R}^{2m} \times \mathbb{R}^{2m} \to \mathbb{R}^{2m}$ defines the boundary conditions. Hereafter, both H and g will be assumed to be suitably regular. For existence and uniqueness results concerning general (not necessarily Hamiltonian) two-point boundary value problems we refer the reader to [22]. As is well known, the value of the Hamiltonian function is constant along the solution of (1). An easy manner to see this is to consider the line integral associated with the vector field $\nabla H(y)$ evaluated along the path defined by the solution $y(t)$ of (1), which equals the variation of H along the end-points of the path. Exploiting the skew-symmetry of matrix J, we have, for $t_0 \le t \le t_f$,

$$\begin{aligned} H(y(t)) - H(y(t_0)) &= \int_{t_0}^{t} \dot{y}^\top(\tau)\nabla H(y(\tau))\mathrm{d}\tau \\ &= \int_{t_0}^{t} \nabla^\top H(y(\tau))J^\top \nabla H(y(\tau))\mathrm{d}\tau = 0. \end{aligned} \tag{2}$$

The state vector y splits in two vectors of length m, $y^\top = [q^\top, p^\top]$ referred to as generalized coordinates and conjugate momenta. The numerical treatment of Hamiltonian problems is thoroughly discussed in the monographs [18, 25, 31].

The aim of the present work is to construct energy-conserving methods for problem (1), that is methods producing numerical solutions $\{y_i\}$ along which the value of the energy is the same: $H(y_i) = H(y_{i-1})$.

Interest in problems such as (1) arises in several research areas. In this paper (see Section 5), we focus our attention on some applications in celestial mechanics and astrodynamics. In particular, we consider the dynamics of a massless object (planetoid) subject to the gravitational field induced by two massive bodies (primaries) revolving in circular orbits about their center of mass. Such a dynamical system, referred to as the *circular restricted three-body problem*, together with its generalizations, has been deeply studied since Poincaré. Its renewed interest is motivated by the fundamental role it plays in the context of space mission design and control problems in aerospace engineering, such as the nonlinear trajectory optimization and the spacecraft orbit transfer [6, 23].

The paper is organized as follows. In the next section we briefly recall the definition of the energy-conserving methods named HBVMs and describe their main features. For a detailed description of HBVMs, and their properties when applied to Hamiltonian IVPs, see [9–11]. The implementation of HBVMs to solve problem (1) are discussed in Sections 3 and 4. In particular, in the latter section we study the more

delicate case of periodic boundary conditions: as is well known, the detection of periodic orbits takes on great importance in the context of Hamiltonian systems. Section 5 is devoted to the description of specific problems related to the circular restricted three-body system, and their numerical treatment. A few concluding remarks are then reported in Section 6. For an introduction on the solution of general boundary value problems by using one-step methods see, for example, [5].

2 Definition of the methods

In this section we recall the definition of HBVMs. These are Runge–Kutta methods characterized by a low-rank coefficient matrix.

The main prerogative of a HBVM is to reproduce, in the discrete setting, property (2) of conservative vector fields. To this end, we consider the approach discussed in [11] and exploit a Fourier expansion of the continuous problem $\dot{y}(t) = J\nabla H(y(t))$ restricted to the interval $t \in [t_0, t_0 + h]$, where $h = \frac{t_f - t_0}{n} > 0$ will act as the stepsize of integration in the one-step method that will finally arise from this analysis. The procedure is then iterated on adjacent intervals $[t_i, t_{i+1}]$ with $t_{i+1} = t_i + h$, $i = 0, \ldots, n-1$, until the overall integration interval $[t_0, t_f]$ is covered.

Let us then consider the *Legendre* polynomials P_i shifted on the interval $[0, 1]$, and scaled in order to be orthonormal:

$$\deg P_i = i, \qquad \int_0^1 P_i(x)P_j(x)\mathrm{d}x = \delta_{ij}, \qquad \forall i, j \geq 0, \tag{3}$$

where δ_{ij} is the Kronecker symbol. The roots $\{c_1, \ldots, c_k\}$ of $P_k(x)$ are all distinct and symmetrically distributed on the interval $(0, 1)$. Usually, they are referred to as the Gauss-Legendre abscissae on $[0, 1]$ and generate the well-known Gauss-Legendre quadrature formulae, whose weights we denote b_i, $i = 1, \ldots, k$. The infinite sequence $\{P_i(t)\}$ forms an orthonormal basis of $L^2([0, 1])$. Expanding the right-hand side of (1) along this basis and truncating the series after s terms changes the original differential equation $\dot{y}(t) = J\nabla H(y(t))$ to

$$\dot{\omega}(t_0 + ch) = \sum_{j=0}^{s-1} P_j(c) \int_0^1 P_j(x) J\nabla H(\omega(t_0 + xh))\mathrm{d}x, \qquad c \in [0, 1]. \tag{4}$$

Notice that the solution $\omega(t_0 + ch)$ of (4) is indeed a polynomial of degree s. In [11, Theorem 1] it has been shown that

$$y(t_0 + h) - \omega(t_0 + h) = O(h^{2s+1}),$$

so that, iterating the procedure (4) sequentially over the intervals $[t_i, t_{i+1}]$, $i = 0, \ldots, n-1$, provides an approximation of order $2s$ to the true solution, on the whole interval $[t_0, t_f]$. One interesting aspect of formula (4) is that it inherits the energy conservation property of the original problem. In fact, by setting

$$\gamma_j(\omega) = \int_0^1 P_j(x) J\nabla H(\omega(t_0 + xh))\mathrm{d}x, \quad j = 0, \ldots, s-1, \tag{5}$$

we have

$$\begin{aligned} H(\omega(t_1)) - H(\omega(t_0)) &= h\int_0^1 \dot{\omega}(t_0+ch)^\top \nabla H(\omega(t_0+ch))\mathrm{d}c \\ &= h\sum_{j=0}^{s-1} \gamma_j(\omega)^\top J^\top \gamma_j(\omega) = 0. \end{aligned} \tag{6}$$

A drawback of formula (4) is the presence of the integrals defining the scalar products (5), which make it unusable for a direct implementation. To circumvent this problem, a quadrature formula is introduced to approximate such integrals. In particular, we consider the Gauss-Legendre quadrature based at $k \geq s$ abscissae c_i and weights b_i, $i = 1, \ldots, k$, introduced earlier, thus obtaining the following approximation to (5):

$$\hat{\gamma}_j(\omega) \equiv \sum_{\ell=1}^{k} b_\ell P_j(c_\ell) J \nabla H(\omega(t_0 + c_\ell h)) = \gamma_j(\omega) + O(h^{2k-j}). \tag{7}$$

In so doing, the polynomial approximation changes, so that we finally arrive at the method

$$y_1 = \Phi_h(y_0) \equiv \sigma(t_0 + h), \tag{8}$$

where the polynomial $\sigma \in \Pi_s$ is defined as (compare with (4))

$$\dot{\sigma}(t_0 + ch) = \sum_{j=0}^{s-1} P_j(c) \sum_{\ell=1}^{k} b_\ell P_j(c_\ell) J \nabla H(\sigma(t_0 + c_\ell h)). \tag{9}$$

It can be shown that this method has still order $2s$ [11, Theorem 4]. However, due to the approximation (7), the polynomial σ does not retain, in general, the conservation property (6) of the original polynomial ω. Nevertheless, this is no much of an issue since the following two situations may occur:

1. $H(y)$ is a polynomial of degree, say ν. In this case, the integrand in (5) has degree at most $\nu s - 1$ and, since the Gauss-Legendre quadrature formula is exact for polynomials of degree at most $2k - 1$, it will be enough to choose $k \geq \frac{\nu s}{2}$ to get $\hat{\gamma}_j = \gamma_j$ and hence energy conservation. Indeed, in such a case one evidently obtains $\omega \equiv \sigma$;
2. $H(y)$ is a general, though suitably regular, non-polynomial function. According to the analysis in [11], one then proves that (see (8)–(9))

$$H(y_1) - H(y_0) = O(h^{2k+1}). \tag{10}$$

Consequently, even in this case, we can get a *practical energy conservation* by choosing k as large as to guarantee that the error $O(h^{2k+1})$, appearing at the right-hand side in (10), is of the order of the machine epsilon. As we will see in the next section, choosing a large k does not affect the overall computational cost associated with the implementation of the method, which essentially depends on s.

Integrating both sides of (9) with respect to the variable c and evaluating at $c = c_i$ yields

$$\sigma(t_0+c_ih) = y_0+h\sum_{j=0}^{s-1}\int_0^{c_i} P_j(\tau)\mathrm{d}\tau \sum_{\ell=1}^{k} b_\ell P_j(c_\ell) J\nabla H(\sigma(t_0+c_\ell h)), \quad i = 1,\dots,k. \tag{11}$$

This formula is called *Hamiltonian Boundary Value Method* (HBVM) and is tantamount to a Runge–Kutta collocation-like method with internal stages $Y_i \equiv \sigma(t_0 + c_ih)$. In fact, by setting

$$\mathcal{P}_s = \begin{pmatrix} P_0(c_1) & \dots & P_{s-1}(c_1) \\ \vdots & & \vdots \\ P_0(c_k) & \dots & P_{s-1}(c_k) \end{pmatrix}, \quad \mathcal{I}_s = \begin{pmatrix} \int_0^{c_1} P_0(x)\mathrm{d}x & \dots & \int_0^{c_1} P_{s-1}(x)\mathrm{d}x \\ \vdots & & \vdots \\ \int_0^{c_k} P_0(x)\mathrm{d}x & \dots & \int_0^{c_k} P_{s-1}(x)\mathrm{d}x \end{pmatrix}$$

$c = (c_1,\dots,c_k)^\top$, $b = (b_1,\dots,b_k)^\top$ and $\Omega = \mathrm{diag}(b_1, b_2, \dots, b_k)$, (8)–(11) is equivalent to the k-stage R-K method defined by the following Butcher tableau:

$$\begin{array}{c|c} c & \mathcal{I}_s\mathcal{P}_s^\top\Omega \\ \hline & b^\top \end{array}. \tag{12}$$

This method is denoted by HBVM(k, s) to outline its dependence on the two integers s (degree of the polynomial approximation, clearly determined by the number of Legendre polynomials involved) and k (which is related to the number of internal abscissae and, therefore, to the order of the quadrature).

Notice that $\mathcal{P}_s$ and $\mathcal{I}_s$ are $k \times s$ matrices while $\Omega \in R^{k\times k}$. When $k = s$ one can show that (12) becomes the usual Gauss collocation method of order $2s$ [9]. For any $k \geq s$ the coefficient matrix $A = \mathcal{I}_s\mathcal{P}_s^\top\Omega$ has constant rank s and its nonzero eigenvalues coincide with those of the Butcher matrix defining the basic s-stage Gauss method [10]. The main properties of HBVMs are summarized in the following theorem (see [11, Corollary 3]).

Theorem 1 *HBVM(k, s) is symmetric, of order $2s$ and energy-conserving for all polynomial Hamiltonians of degree $\nu \leq \frac{2k}{s}$. In any other case, $H(y_1) - H(y_0) = O(h^{2k+1})$, provided that H is suitably regular.*

3 Simplified Newton iteration and implementation details

That the rank of the coefficient matrix $\mathcal{I}_s\mathcal{P}_s^\top\Omega$ is s, independently of k, suggests that $k - s$ stages Y_i may be regarded as linear combinations of the remaining s stages. This algebraic property turns out to be of fundamental importance to reduce the computational effort associated with the implementation of the method when applied to (1). Therefore, it is convenient to derive an alternative (though equivalent) shape of an HBVM(k, s) method.

Notice that the polynomial σ in (9) has degree s. Hence, it is completely determined by s (rather than k) stages, plus the condition $\sigma(t_0) = y_0$. These s stages

have been called *fundamental stages* and, without loss of generality, in order to maintain the notation as simple as possible, they are assumed to be the first ones: Y_i, $i = 1, \dots, s$.[1] The remaining stages Y_j, $j = s+1, \dots, k$, though contributing in defining the final shape of the polynomial σ, may be conveniently defined as linear combinations of the fundamental stages, by simply setting $Y_j = \sigma(t_0 + c_j h)$. In other words, setting $Z \equiv (Y_1^\top, \dots, Y_s^\top)^\top$, $W \equiv (Y_{s+1}^\top, \dots, Y_k^\top)^\top$, we have

$$W = a_0 \otimes y_0 + A \otimes I_{2m} Z, \tag{13}$$

where the entries of the vector $a_0 \in \mathbb{R}^{k-s}$ and the matrix $A \in \mathbb{R}^{(k-s)\times s}$ are the evaluations, at the abscissae $c_{s+1}, \dots, c_k$, of the Lagrange polynomials defined on the nodes $\{0, c_1, \dots, c_s\}$. For this reason, the stages in W have been referred to as *silent stages* [20]. In conclusion, we arrive at the following formulation of the method

$$\begin{cases} -e \otimes y_0 + Z = h(B_1 \otimes J)\nabla H(Z) + h(B_2 \otimes J)\nabla H(W), \\ W = a_0 \otimes y_0 + A \otimes I_{2m} Z, \\ -y_0 + y_1 = h(\beta_1^\top \otimes J)\nabla H(Z) + h(\beta_2^\top \otimes J)\nabla H(W), \end{cases} \tag{14}$$

where the first block-equation corresponds to the first s equations in (11) (so matrix $[B_1, B_2]$ is composed by the first s rows of the Butcher array $\mathcal{I}_s \mathcal{P}_s^\top \Omega$ in (12)), the second block-equation, defining the silent stages, is inherited from (13), and the last equation defines the new approximation, y_1, having set $\beta_1 = [b_1, \dots, b_s]^\top$ and $\beta_2 = [b_{s+1}, \dots, b_k]^\top$. The clear advantage of (14), with respect to (12), is that now the nonlinear and linear parts of the system defining the stages are completely uncoupled.

Suppose that the interval $[t_0, t_f]$ is divided into n equispaced sub-intervals $[t_{i-1}, t_i]$, $i = 1, \dots, n$, of length h. Then, Eq. 14 may be subsequently iterated on such intervals to yield the approximations $y_i \simeq y(t_i)$, for $i = 0, \dots, n$. In particular, $y_0, y_1, \dots, y_n$ are combined with the given boundary conditions to yield a large nonlinear system in the unknowns $y_0, Z_0, y_1, Z_1, \dots, y_{n-1}, Z_{n-1}, y_n$, where Z_i is the block-vector of the fundamental stages (denoted by Z in the first equation of (14)) associated with y_i.

Ignoring momentarily the boundary conditions, a Newton-like iteration applied to the nonlinear equations gives the sequences $\{y_i^{(j)}\}$ and $\{Z_i^{(j)}\}$ defined as

$$\begin{aligned} y_i^{(j+1)} &= y_i^{(j)} + \delta_i^{(j)}, \qquad \text{for } i = 0, \dots, n, \\ Z_i^{(j+1)} &= Z_i^{(j)} + \Delta_i^{(j)}, \qquad \text{for } i = 0, \dots, n-1, \end{aligned}$$

[1] In the actual implementation, their distribution is chosen according to what explained in [7] (see also [8]), i.e., the corresponding s abscissae are approximately uniformly spaced in $[0, 1]$.

where the increments $\delta_i^{(j)}$ on the y_i variable and $\Delta_i^{(j)}$ on the Z_i variable are the solution of the following linear system with sparse structured coefficient matrix:

$$\begin{pmatrix} V_1 & K_1 & & & & & \\ L_1 & U_1^\top & I_{2m} & & & & \\ & V_2 & K_2 & & & & \\ & L_2 & U_2^\top & I_{2m} & & & \\ & & \ddots & \ddots & & & \\ & & & & V_n & K_n & \\ & & & & L_n & U_n^\top & I_{2m} \end{pmatrix} \begin{pmatrix} \delta_0^{(j)} \\ \Delta_0^{(j)} \\ \delta_1^{(j)} \\ \Delta_1^{(j)} \\ \delta_2^{(j)} \\ \vdots \\ \delta_{n-1}^{(j)} \\ \Delta_{n-1}^{(j)} \\ \delta_n^{(j)} \end{pmatrix} = \begin{pmatrix} \theta_1 \\ \Theta_1 \\ \theta_2 \\ \Theta_2 \\ \vdots \\ \theta_n \\ \Theta_n \end{pmatrix}. \tag{15}$$

The blocks $V_i, U_i \in \mathbb{R}^{2ms\times 2m}$, $L_i \in \mathbb{R}^{2m\times 2m}$ and $K_i \in \mathbb{R}^{2ms\times 2ms}$ are defined as follows:[2]

$$\begin{aligned} V_i &= -e \otimes I_{2m} - h(B_2 a_0) \otimes J\nabla^2 H(\bar{y}_i^{(j)}), \\ U_i^\top &= -h(\beta_2^\top A + \beta_1^\top) \otimes J\nabla^2 H(\bar{y}_i^{(j)}), \\ L_i &= -I_{2m} - h(\beta_2^\top a_0) J\nabla^2 H(\bar{y}_i^{(j)}), \\ K_i &= I_s \otimes I_{2m} - h(B_2 A + B_1) \otimes J\nabla^2 H(\bar{y}_i^{(j)}), \end{aligned} \tag{16}$$

where, for symmetry reasons, $\bar{y}_i^{(j)} = \frac{y_i^{(j)} + y_{i-1}^{(j)}}{2}$. Finally, $\theta_i \in \mathbb{R}^{2m}$ and $\Theta_i \in \mathbb{R}^{2ms}$ are the right-hand sides of the Newton-like iteration computed from (14).

Remark 1 If $k = s$, that is when using the s-stage Gauss-Legendre method, the definition of the blocks in (16) simplifies since the terms involving B_2 and β_2 disappear. Thus, for example, $V_i = -e \otimes I_{2m}$ and $L_i = -I_{2m}$. Nevertheless, when $k > s$, the overhead is marginal, also taking into account that the terms $B_2 a_0$, $\beta_2^\top A + \beta_1^\top$, $\beta_2^\top a_0$ and $B_2 A + B_1$ may be precomputed at the very beginning of the process.

We notice that system (15) counts $2m(s+1)n$ equations in $2m(s+1)n + 2m$ unknowns, thus we need $2m$ extra equations that will be derived by imposing the boundary conditions. Clearly, we shall obtain different linear systems, depending on the boundary conditions in (1): generally, their efficient solution requires the use of different, specifically tailored, linear solvers. This particular aspect is only sketched here and will be considered elsewhere.

Preliminarily, we observe that simple matrix manipulations would allow us to separate the computation of the stages updates $\Delta_i^{(j)}$ from the solution updates $\delta_i^{(j)}$. In fact, if K_i is nonsingular, from (15) one easily derives that

$$\Delta_{i-1}^{(j)} = K_i^{-1}(\theta_i - V_i \delta_{i-1}^{(j)}), \quad i = 1, \ldots, n.$$

[2] In order not to complicate the notation, and for sake of brevity, we shall omit the iteration index j, for these blocks and for the known coefficients at the right hand side of (15). We will do the same in formula (41).

However, due to possible stability problems (indeed, K_i may be ill conditioned or even singular), in general it is preferable to avoid this reduction step.

Regarding the solvability and the efficient solution of (15) coupled with separated or non-separated but non-periodic boundary conditions, we refer to [5, Chapter 8] and [13, Chapter 7]. We sketch these two cases in Sections 3.1 and 3.2, respectively.

The case of periodic boundary conditions is far more involved. In fact, periodic orbits of Hamiltonian systems are not isolated and, consequently, much care must be taken to define a well-posed discrete problem and to analyze the properties of its solution. For these reasons, we devote Section 4 to discuss this important case in greater detail.

3.1 Separated boundary conditions

The simplest case is when problem (1) is defined by means of $r < 2m$ initial and $2m - r$ final nonlinear conditions:

$$g_1(y_0) = 0 \in \mathbb{R}^r, \qquad g_2(y_n) = 0 \in \mathbb{R}^{2m-r}.$$

Their linearization, which is needed during the Newton process, provides additional equations in the form

$$G_1\delta_0^{(j)} = g_1(y_0^{(j)}) \in \mathbb{R}^r, \qquad G_2\delta_n^{(j)} = g_2(y_n^{(j)}) \in \mathbb{R}^{2m-r}, \tag{17}$$

where $G_1 \in R^{r\times 2m}$ and $G_2 \in R^{(2m-r)\times 2m}$. Ordering the two equations as the first and the last one, (15) and (17) produce a linear system with an *Almost Block Diagonal* (ABD) coefficient matrix [2]. In such a case, the solution is efficiently obtained by means of direct solvers that generalize the LU factorization (see [2] for a complete review), with a computational cost consisting into a number of operations proportional to m^2s^2n and no fill-in (i.e., no additional memory is required for the factorization, besides that needed for storing the blocks in the coefficient matrix).

3.2 Non-separated boundary conditions

Suppose problem (1) is defined by means of $2m$ (generally nonlinear) boundary conditions involving y_0 and y_n, i.e.,

$$g(y_0, y_n) = 0 \in \mathbb{R}^{2m}.$$

Then, the linearization of this condition produces an equation of the form

$$G_1\delta_0^{(j)} + G_2\delta_n^{(j)} = g(y_0^{(j)}, y_n^{(j)}) \in \mathbb{R}^{2m}, \tag{18}$$

that, combined with (15), gives a nonsingular *Bordered Almost Block Diagonal* (BABD) linear system whose factorization is conveniently handled by means of a cyclic reduction approach, as is shown in [3]. This algorithm requires twice the number of operations as in the previous case and generates a fill-in which is essentially equal to $2m(2m + s)n$ memory locations [3].

4 Periodic boundary conditions

From a numerical point of view, the most difficult case to be solved is when problem (1) is defined with periodic boundary conditions, i.e.,

$$g(y_0, y_n) \equiv y_0 - y_n = 0. \tag{19}$$

As is the case with general (not necessarily Hamiltonian) autonomous systems, the continuous problem always admits an infinite number of solutions: the phase of the solution is always undetermined, meaning that y_0 could be any point on the given periodic orbit.

Conservation of energy in canonical Hamiltonian systems adds a further, more subtle, source of indeterminacy which reflects the fact that periodic orbits are not isolated. A periodic solution typically lies in a $(2m-1)$-dimensional level set of the energy, and thus in nearby level sets there are other periodic orbits (think of close orbits around a stationary point). However, they may be isolated in a given energy level set. Hereafter we elucidate in more detail the genesis of the above-mentioned issues and how they are accounted for. This preliminary analysis is carried out in the continuous setting and will be exploited later to state convergence and energy-preserving results for the considered methods.

Let $y_0 \in \mathbb{R}^{2m}$ and denote by φ_t the flow associated with the dynamical system $\dot{y}(t) = J\nabla H(y(t))$ coupled with the initial condition $y(0) = y_0$, namely $\varphi_t(y_0) \equiv y(t)$.[3] We denote by $\bar{y}(t)$ a given periodic orbit of period T and choose $\bar{y}_0 = \bar{y}(0)$, thus $\varphi_t(\bar{y}_0) = \bar{y}(t)$. As is well known, the Jacobian matrix $\Phi(t) = \frac{\partial \varphi_t(\bar{y}_0)}{\partial \bar{y}_0}$ is the fundamental matrix solution for the linearized equation about the periodic orbit $\bar{y}(t)$ and satisfies the variational problem

$$\begin{cases} \dot{\Phi}(t) = J\nabla^2 H(\varphi_t(\bar{y}_0))\Phi(t), \\ \Phi(0) = I. \end{cases} \tag{20}$$

In particular, matrix $\Phi(T)$ is referred to as *monodromy matrix* and represents the state transition matrix after one period, while its eigenvalues λ_i are called *Floquet* or *characteristic multipliers* and have the form $\lambda_i = e^{\sigma_i T}$, σ_i being the characteristic exponents.

The monodromy matrix of a Hamiltonian system is symplectic, that is $\Phi(T)^\top J \Phi(T) = J$. This implies that $\Phi(T)^\top$ is similar to $\Phi^{-1}(T)$ and, consequently, the characteristic multipliers appear in either pairs $\lambda, \bar{\lambda}$ if $|\lambda| = 1$, or quadruples $\lambda, \bar{\lambda}, \lambda^{-1}, \bar{\lambda}^{-1}$ if $|\lambda| \neq 1$. In particular, a unitary multiplier must necessarily have even algebraic multiplicity.

The monodromy matrix plays an important role in analyzing the stability properties of periodic orbits and, in our context, in deriving existence and uniqueness results as well as convergence properties of the iteration scheme we will use to compute a periodic orbit numerically. In fact, detecting a periodic orbit $\bar{y}(t)$ requires the solution of the nonlinear system

$$F(y_0, t) \equiv y_0 - \varphi_t(y_0) = 0, \tag{21}$$

[3] Without loss of generality, we assume $t_0 = 0$ here and in the sequel.

in the unknowns y_0 and t. A study of the solutions of (21) in a neighborhood of $(\bar{y}_0, T)$ as well as the stability of the periodic orbit $\bar{y}(t)$, requires a spectral analysis of $F'(z)$ evaluated at $(\bar{y}_0, T)$ and hence of matrix $\Phi(T)$. It turns out that

$$F'(\bar{y}_0, T) = (I - \Phi(T), -J\nabla H(\bar{y}_0)), \tag{22}$$

and the implicit function theorem cannot be applied since $I - \Phi(T)$ has a rank deficiency at least 2 as a consequence of the following well known result (for completeness, we report the short proof since it provides a formula that will be useful in the subsequent discussion).

Lemma 1 [23, Section 4.3] *Matrix $\Phi(T)$ admits $\lambda = 1$ as an eigenvalue with algebraic multiplicity at least 2.*

Proof Let $\bar{y}(t)$ be a T-periodic solution with $\bar{y}(0) = \bar{y}_0$. Differentiating $\dot{\bar{y}}(t) = J\nabla H(\bar{y}(t))$ with respect to t yields $\ddot{\bar{y}}(t) = J\nabla^2 H(\bar{y}(t))\dot{\bar{y}}(t)$. Thus $\dot{\bar{y}}(t)$ solves the variational problem (20) and therefore may be cast as $\dot{\bar{y}}(t) = \Phi(t)\dot{\bar{y}}(0) = \Phi(t)(J\nabla H(\bar{y}_0))$. Notice that $\dot{\bar{y}}(t)$ is also T-periodic and consequently

$$\Phi(T)(J\nabla H(\bar{y}_0)) = J\nabla H(\bar{y}_0). \tag{23}$$

Since $\Phi(T)$ is symplectic, the characteristic multiplier $\lambda = 1$ has even multiplicity. □

Notice that the symplecticity of $\Phi(T)$ and (23) imply

$$\nabla^\top H(\bar{y}_0)\Phi(T) = \nabla^\top H(\bar{y}_0), \tag{24}$$

that is, $\nabla^\top H(\bar{y}_0)$ is a left eigenvector of $\Phi(T)$.

Relations (23) and (24) are responsible for the indeterminacies arising from the time-shift symmetry and energy conservation respectively. It is possible to show that, for any additional non-degenerate first integral $L(y)$, the vector $\nabla L^\top(\bar{y}_0)$ is again a left eigenvector of $\Phi(T)$ associated with the eigenvalue 1 [27].[4] In this paper, consistently with the examples discussed in Section 5, we assume that there are no independent first integrals other than the Hamiltonian function itself. In particular, ordering the eigenvalues of $\Phi(T)$ as $\lambda_1 = \lambda_2 = 1, \lambda_3, \ldots, \lambda_{2m}$, we assume that $\lambda_i \neq 1$ for $i = 3, \ldots, 2m$, in which case the periodic orbit $\bar{y}(t)$ is called *elementary*. Moreover, we shall hereafter assume that the geometric muliplicity of the unit eigenvalue is one.[5]

To remove the non-uniqueness caused by time shift symmetry, one adds an extra scalar equation to (21) representing a section Σ transverse to the periodic orbit at $\bar{y}_0$ (Poincaré section). We will choose a Poincaré section orthogonal to the periodic orbit

[4] A first integral $L(y)$ is non-degenerate if $\nabla L(y)$ does not vanish on the periodic orbit. This is always the case with ∇H, since $\nabla H(\bar{y}_0) = 0$ would imply that $\bar{y}_0$ is an equilibrium.

[5] This is the case of the problems considered for the numerical tests in Section 5 (see, e.g., [17]). More in general, this is true for problems admitting only one first integral, and possessing the so called *scaling property* (see [27] for details).

at $\bar{y}_0$:

$$\Sigma = \left\{ y_0 \,|\, (J\nabla H(\bar{y}_0))^\top (y_0 - \bar{y}_0) = 0 \right\} \;\Leftrightarrow\; \Sigma = \bar{y}_0 + \mathrm{span}(J\nabla H(\bar{y}_0))^\perp. \quad (25)$$

The study of the dynamics around the periodic orbit $\bar{y}(t)$ is carried out by analyzing the nature of the fixed point $\bar{y}_0$ of the first return map

$$P = y_0 \in \Sigma \mapsto \varphi_{T(y_0)}(y_0) \in \Sigma,$$

where $T(y_0)$ is the first return time.

To remove the non-uniqueness caused by energy conservation, one intersects the Poincaré section Σ with an energy level set, say

$$H(y_0) = H_0, \quad (26)$$

where H_0 is the energy value we are interested in. We denote by Σ_{H_0} this intersection and by P_{H_0} the restriction of P to Σ_{H_0}. It turns out that the eigenvalues of the Jacobian matrix $\frac{\partial P_{H_0}(y_0)}{\partial y_0}|_{y_0=\bar{y}_0}$ associated with the return map linearized in a neighborhood of $\bar{y}_0$ are $\lambda_3, \ldots \lambda_{2m}$ and, in view of the foregoing assumption, we conclude that $\bar{y}_0$ and hence $\bar{y}(t)$ are isolated, which means that the augmented system (21)-(25)-(26) does not admit solutions other than $(\bar{y}_0, T_0)$ in a neighborhood of $\bar{y}_0$. In particular, the following important result holds true [26, Theorem 8.5.1]

Theorem 2 (The cylinder theorem) *An elementary periodic orbit of a system with integral H lies in a smooth cylinder of periodic solutions parameterized by the integral.*

Thus it makes sense to detect a periodic orbit by exploiting its energy value, which makes the use of energy-preserving methods particularly appealing.

A standard way to solve (21)-(25)-(26) is via a Newton-like iteration. However, linearizing this system would produce a family of overdetermined linear systems ($2m+1$ unknowns vs. $2m+2$ equations). To avoid handling overdetermined systems and the singularity issues described in Lemma 1, an extra auxiliary unknown μ is usually introduced, which will not affect the final result (see, e.g. [15, 32, 34]). More specifically, we add the unfolding term $\mu\nabla H(y)$ to the original Hamiltonian system, so it becomes

$$\dot{y} = J\nabla H(y) + \mu\nabla H(y) = (J + \mu I)\nabla H(y), \quad (27)$$

where μ is a real parameter. A solution $y(t)$ of (27) satisfies

$$\dot{H}(y(t)) = \nabla H^\top(y(t))(J\nabla H(y(t)) + \mu\nabla H(y(t))) = \mu||\nabla H(y(t))||_2^2. \quad (28)$$

It follows that if $y(t)$ is not an equilibrium point, $H(y(t))$ is constant if and only if $\mu = 0$. Thus, the periodic solution $\bar{y}(t)$ of the original Hamiltonian system $\dot{y} = J\nabla H(y)$ may be computed by searching for periodic solutions of the parametric dynamical system (27). Working with (27) not only has the advantage to lead to a nonsingular family of linear systems during the implementation of the Newton scheme, but also allows us to state the energy-preserving properties of HBVMs applied in this context (see Theorem 2 below). First of all, we show that a HBVM applied to (27) satisfies a property analogous to (28).

Lemma 2 *Let y_0 be a generic non-stationary initial condition. The numerical solution y_1 computed by a HBVM applied to (27) on the time interval $t \in [t_0, t_0 + h]$ satisfies*

$$H(y_1) = H(y_0) \quad \Leftrightarrow \quad \mu = 0. \tag{29}$$

It follows that for a HBVM, a numerical periodic solution $y_0, y_1, \ldots y_n = y_0$ of the original Hamiltonian system may be also computed by searching for numerical periodic solutions of the parametric system (27).

Proof For simplicity (but without loss of generality) we assume that the condition listed in item 1. of Section 2 holds true.[6] This allows us to exchange σ with ω (see (4) and (9)). The polynomial ω is now defined as

$$\dot\omega(t_0+ch) = \sum_{j=0}^{s-1} P_j(c) \int_0^1 P_j(x)(J+\mu I)\nabla H(\omega(t_0+xh))\mathrm{d}x, \qquad c \in [0,1], \tag{30}$$

so that, repeating the calculation in (6) for the problem at hand gives

$$\begin{aligned}
H(\omega(t_1)) - H(\omega(t_0)) &= h\int_0^1 \dot\omega(t_0+ch)^\top \nabla H(\omega(t_0+ch))\mathrm{d}c \\
&= h\int_0^1 \left(\sum_{j=0}^{s-1} P_j(c)\int_0^1 P_j(x)(J+\mu I)\nabla H(\omega(t_0+xh))\mathrm{d}x\right)^\top \nabla H(\omega(t_0+ch))\mathrm{d}c \\
&= h\sum_{j=0}^{s-1}\left(\int_0^1 P_j(x)\nabla H(\omega(t_0+xh))\mathrm{d}x\right)^\top (J^\top+\mu I)\left(\int_0^1 P_j(c)\nabla H(\omega(t_0+ch))\mathrm{d}c\right) \\
&= h\mu\sum_{j=0}^{s-1}\left\|\int_0^1 P_j(x)\nabla H(\omega(t_0+xh))\mathrm{d}x\right\|_2^2.
\end{aligned} \tag{31}$$

The claim follows by observing that the last sum in (31) is strictly positive. In fact, suppose (by contradiction) that $\int_0^1 P_j(x)\nabla H(\omega(t_0+xh))\mathrm{d}x = 0$ for all $j = 0, \ldots, s-1$. Then, from (30), we would get $\dot\omega(t_0+ch) = 0$ for $c \in [t_0, t_0+ch]$ and hence $\omega(t_0) = y_0$ would be an equilibrium point. □

In the sequel, we continue to maintain the same notation for the flow and the monodromy matrix associated with the perturbed problem (27). Nonetheless, we make the presence of the parameter μ explicit by adding it as an extra argument in the functions involved in the next computations. For example, $\varphi_t(y_0, \mu)$ will denote the flow associated with the perturbed problem (27), so $\varphi_t(y_0, 0)$ becomes the flow $\varphi_t(y_0)$ of the original unperturbed Hamiltonian system, and so on. In particular, Eq. 21 becomes

$$F(y_0, t, \mu) \equiv y_0 - \varphi_t(y_0, \mu) = 0. \tag{32}$$

[6] Should this condition not be satisfied, we could always choose k large enough to make the reasoning still valid (see item 2. of Section 2).

Set

$$G(y_0, t, \mu) = \begin{pmatrix} F(y_0, t, \mu) \\ (J\nabla H(\bar{y}_0))^\top (y_0 - \bar{y}_0) \\ H(y_0) - H_0 \end{pmatrix}. \tag{33}$$

The periodic solution $\bar{y}(t)$ is detected by solving $G(y_0, t, \mu) = 0$. A standard way to solve this nonlinear system is via the Newton iteration

$$\begin{cases} G'(z^{(j)})\eta^{(j)} = -G(z^{(j)}), \\ z^{(j+1)} = z^{(j)} + \eta^{(j)}, \end{cases} \tag{34}$$

where $z \equiv (y_0, t, \mu)$, $z^{(j)} \equiv \left(y_0^{(j)}, t^{(j)}, \mu^{(j)}\right)$ is the jth step approximation to the solution, say $\bar{z} \equiv (\bar{y}_0, T, 0)$, of (33) and

$$G'(z) \equiv G'(y_0, t, \mu) = \begin{pmatrix} I - \Phi(t, \mu) & -J\nabla H(\varphi_t(y_0, \mu)) & \frac{\partial \varphi_t}{\partial \mu}(y_0, \mu) \\ (J\nabla H(\bar{y}_0))^\top & 0 & 0 \\ \nabla^\top H(y_0) & 0 & 0 \end{pmatrix}. \tag{35}$$

Under regularity assumptions on the Hamiltonian function, the Newton process is well defined in a neighborhood of $\bar{z}$ and a local quadratic convergence of the sequence $z^{(j)}$ towards $\bar{z}$ is guaranteed provided $G'(\bar{z})$ is nonsingular.

Lemma 3 *Let $\bar{y}_0 \in \mathbb{R}^{2m}$ and $\varphi_t(\bar{y}_0)$ be a periodic orbit with period $T > 0$ (so $\nabla H(\bar{y}_0) \neq 0$). Then, the matrix*

$$G'(\bar{y}_0, T, 0) = \begin{pmatrix} I - \Phi(T) & -J\nabla H(\bar{y}_0) & \frac{\partial \varphi_T}{\partial \mu}(\bar{y}_0, \mu)|_{\mu=0} \\ (J\nabla H(\bar{y}_0))^\top & 0 & 0 \\ \nabla^\top H(\bar{y}_0) & 0 & 0 \end{pmatrix} \tag{36}$$

is nonsingular.

Proof We split the proof in the following two steps:

(a) we first show that the first block-row in (36) has full rank $2m$;
(b) finally, upon observing that the last two rows are orthogonal, we show that these rows are linearly independent of the first $2m$ rows.

Step (a). The bulk of this part of the proof may be found in [34] but is reported here for completeness. We recall that the double eigenvalue $\lambda = 1$ of $\Phi(T)$ has been assumed to be not semi-simple, so $\lambda = 0$ is not a semi-simple eigenvalue of $I - \Phi(T)$ and brings a single left eigenvector, $\nabla^\top H(\bar{y}_0)$ (see (24)), and right eigenvector, $J\nabla H(\bar{y}_0)$ (see (23)). Consequently, the only possibility for the first $2m$ rows of $G'(\bar{y}_0, T, 0)$ to be linearly dependent

is that $\nabla^\top H(\bar{y}_0)\frac{\partial \varphi_T}{\partial \mu}(\bar{y}_0,\mu)|_{\mu=0}$ vanishes. This is not the case, in fact

$$\begin{aligned}
\nabla^\top H(\bar{y}_0)\frac{\partial \varphi_T}{\partial \mu}(\bar{y}_0,\mu)|_{\mu=0} &= \frac{\partial}{\partial \mu} H(\varphi_T(\bar{y}_0,\mu))|_{\mu=0} \\
&= \frac{\partial}{\partial \mu}\left(H(\bar{y}_0) + (H(\varphi_T(\bar{y}_0,\mu)) - H(\bar{y}_0))\right)|_{\mu=0} \\
&= \frac{\partial}{\partial \mu}\left(H(\bar{y}_0) + \int_0^T \nabla^\top H(\varphi_t(\bar{y}_0,\mu))\,\dot{\varphi}_t(\bar{y}_0,\mu)\mathrm{d}t\right)\Big|_{\mu=0} \\
&= \frac{\partial}{\partial \mu}\left(H(\bar{y}_0) + \int_0^T \mu\|\nabla H(\varphi_t(\bar{y}_0,\mu))\|_2^2\mathrm{d}t\right)\Big|_{\mu=0} \\
&= \int_0^T \|\nabla H(\varphi_t(\bar{y}_0,0))\|_2^2\mathrm{d}t \;\neq\; 0.
\end{aligned}$$

Step (b). First, we notice that

$$\mathrm{Im}(I-\Phi(T)) = \mathrm{Ker}(I-\Phi(T)^\top)^\perp = \mathrm{span}\{\nabla H(\bar{y}_0)\}^\perp. \tag{37}$$

Let z be the right generalized eigenvector $\Phi(T)$ associated with the eigenvalue $\lambda = 1$, namely $(I-\Phi(T))z = J\nabla H(\bar{y}_0)$. From item (a) above we deduce that the kernel of the first block-row in (36) has dimension two and its basis is formed by the two vectors $w_1 = ((J\nabla H(\bar{y}_0))^\top, 0, 0)^\top$ and $w_2 = (z^\top, 1, 0)^\top$. Since $\lambda = 1$ does not admit any further generalized eigenvectors, it follows that $z \notin \mathrm{Im}(I-\Phi(T))$ and consequently, from (37), $\nabla^\top H(\bar{y}_0)z \neq 0$.

With the aid of these preparatory results, a direct computation shows that no linear combination of $w1$ and $w2$ lies in the kernel of $G'(\bar{y}_0, T, 0)$, which is therefore nonsingular.

This completes the proof. □

In view of the fact that the flow is to be replaced by the numerical method, it is useful to extend the above approach, referred to as *single shooting*, to the *multiple shooting* variant [12, 34], for which problem (32) becomes

$$0 = F(y_0, y_1, \ldots, y_{n-1}, h, \mu) \equiv \begin{cases} y_i - \varphi_h(y_{i-1}, \mu), & i = 1, \ldots, n-1, \\ y_0 - \varphi_h(y_{n-1}, \mu), \end{cases} \tag{38}$$

where $h = \frac{t}{n}$ is the stepsize and we have considered the boundary condition (19).

Evidently, system (38), coupled with (25) and (26) admits the solution $(\bar{y}(t_0), \bar{y}(t_1), \ldots \bar{y}(t_{n-1}), \frac{T}{n}, 0)$, where $t_i = ih$. An argument similar to that in the proof of Lemma 3 may be then exploited to deduce that the Newton iteration applied to (38) is convergent for sufficiently good initial data and stepsize h small enough.

We are now in the position to state the main result of the present section.

Theorem 3 *Let y_0 be a generic non-stationary initial condition for problem (27). Consider the nonlinear system*

$$0 = \widehat{F}(y_0, y_1, \ldots, y_{n-1}, h, \mu) \equiv \begin{cases} y_i - \Phi_h(y_{i-1}, \mu), & i = 1, \ldots, n-1, \\ y_0 - \Phi_h(y_{n-1}, \mu), \end{cases} \tag{39}$$

formally defined by replacing the continuous flow φ_h in (38) by its discrete approximation Φ_h obtained by a HBVM(k, s) method, as defined at (8)–(9), with k large enough. Then, for n sufficiently large:

(a) system (39) admits a unique solution $(\bar{y}_0, \bar{y}_1, \ldots \bar{y}_{n-1}, \bar{h}, 0)$;
(b) the Newton method applied to (39) converges locally and quadratically to such a solution;
(c) $H(\bar{y}_i) = H(\bar{y}_0)$, for $i = 1, \ldots, n-1$ (energy conservation).

Proof Again, without loss of generality, we assume that the condition introduced in item 1. of Section 2 holds true. Under regularity assumptions, Φ_h is locally an approximation of order $2s+1$ to φ_h, thus

$$\left\| \widehat{F}(\bar{y}(t_0), \bar{y}(t_1), \ldots, \bar{y}(t_{n-1}), \tfrac{T}{n}, 0) \right\|_\infty = O\left(\left(\tfrac{T}{n}\right)^{2s+1} \right).$$

Using $Y_0 = (\bar{y}(t_0), \bar{y}(t_1), \ldots, \bar{y}(t_{n-1}), \frac{T}{n}, 0)$ as initial condition for the Newton scheme allows us to apply the Newton-Kantorovich theorem [13, 24] to deduce the existence and uniqueness of a solution $\overline{Y} = (\bar{y}_0, \bar{y}_1, \ldots \bar{y}_{n-1}, \bar{h}, \bar{\mu})$ of system (39). We prove that actually $\bar{\mu} = 0$, as indicated at point (a). By definition, the numerical solution $\overline{Y}$ is periodic, thus $H(\bar{y}_0) = H(\bar{y}_n)$, with $\bar{y}_n = \Phi_h(\bar{y}_{n-1}, \bar{\mu})$. From Lemma (2) it then follows that $\bar{\mu} = 0$ and (c) is satisfied. □

4.1 Implementation details

In actual computations, $\bar{y}_0$ is not known a priori and condition (25) is usually replaced by a linear equation, called *anchor* [28], of the form

$$b_a^\top y_0 = b_0, \tag{40}$$

with $b_a \in \mathbb{R}^{2m}$. Notice that, as is the case with (25), Eq. 40 represents a $2m-1$ dimensional hyperplane in $\mathbb{R}^{2m}$. In general, such a hyperplane is not locally orthogonal to the orbit but it is assumed that it acts as a transverse Poincaré section, in which case the result presented in Lemma 3 still holds true. The choice of b_a is often dictated by the symmetry properties of the problem at hand: in most relevant cases the Poincaré section (40) is parallel to a coordinate plane, that is $b_a = e_\ell = (0, \ldots, 1, \ldots, 0)^\top$, the ℓth vector of the canonical basis of $\mathbb{R}^{2m}$. This is the choice we make for detecting periodic orbits of the problems presented in the next section, and one can easily argue that for these specific periodic orbits (25) and (40) do indeed coincide. A more sophisticated technique proposed in [12] consists in avoiding the explicit use of a Poincaré section and thus neglecting the second component in Eq. 33. The undetermined linear systems generated during the Newton process are then solved by exploiting the Moore-Penrose pseudo-inverse of $G'(z^{(j)})$. Under convergence

hypotheses, the resulting sequence $z^{(j)}$, for j large, may be shown to lie in a Poincaré section approximating (25) (see also [34, Remark 2.4]).

To obtain the linear system at the corresponding j-th Newton-like iteration, we observe that:

- in (14), matrix J must be replaced by $J + \mu I$, since the HBVM(k, s) method is now applied to system (27);
- according to (39), the unknown $\delta_n^{(j)}$ can be removed by virtue of (19) and, consequently, also the block-row corresponding to (19) itself;
- the two equations (26) and (40) enter the system;
- the update $\delta_h^{(j)}$, such that $h_{j+1} = h_j + \delta_h^{(j)}$, must be included, where h_j is the current approximation to the unknown value of the correct stepsize $\bar{h}$;
- due to the presence of the variable μ in the system (see (27)), an analogous update $\delta_\mu^{(j)}$, such that $\mu_{j+1} = \mu_j + \delta_\mu^{(j)}$, must be included.

Consequently, the linear system generated by the Newton-type iteration assumes the form

$$\begin{pmatrix}
b_H^\top & & & & & & & & & \\
b_a^\top & & & & & & & & & \\
V_1 & K_1 & & & & & & & v_1 & w_1 \\
L_1 & U_1^\top & I_{2m} & & & & & & \hat{v}_1 & \hat{w}_1 \\
 & & V_2 & K_2 & & & & & v_2 & w_2 \\
 & & L_2 & U_2^\top & I_{2m} & & & & \hat{v}_2 & \hat{w}_2 \\
 & & & & \ddots & \ddots & & & \vdots & \\
 & & & & & & V_n & K_n & v_n & w_n \\
I_{2m} & & & & & & L_n & U_n^\top & \hat{v}_n & \hat{w}_n
\end{pmatrix}
\begin{pmatrix}
\delta_0^{(j)} \\ \Delta_0^{(j)} \\ \delta_1^{(j)} \\ \Delta_1^{(j)} \\ \delta_2^{(j)} \\ \vdots \\ \delta_{n-1}^{(j)} \\ \Delta_{n-1}^{(j)} \\ \delta_h^{(j)} \\ \delta_\mu^{(j)}
\end{pmatrix}
=
\begin{pmatrix}
\gamma_1 \\ \gamma_2 \\ \theta_1 \\ \Theta_1 \\ \theta_2 \\ \Theta_2 \\ \vdots \\ \theta_n \\ \Theta_n
\end{pmatrix}, \tag{41}$$

where: $b_H^\top = \nabla^\top H(y_0^{(j)})$, $b_a^\top \in \mathbb{R}^{1\times 2m}$, and $\gamma_1, \gamma_2 \in \mathbb{R}$ derive from the linearization of (26) and (40), respectively; blocks $V_i, U_i^\top, L_i, K_i$ are the same as defined in (16) but with h_j in place of h and $J + \mu I$ in place of J; v_i and $\hat{v}_i$ are vectors of suitable dimension obtained by differentiating (14) with respect to h; analogously, the vectors w_i and $\hat{w}_i$ are obtained by differentiating (14) with respect to μ.

The solution of system (41) can be efficiently computed by using an algorithm similar to that considered for non-separated boundary conditions [2, 3].

We finally observe that, under the assumptions listed below formula (24), we have a result analogous to Theorem 1 but using the period T instead of the energy value as a parameter for the family of periodic orbits. A periodic orbit with a given period $\overline{T}$ may be computed by removing the equation corresponding to (26) from (41) and considering that now the stepsize $h = \frac{\overline{T}}{n}$ must no longer be treated as an unknown.

In the numerical experiments illustrated in the next section we outline some potentialities of dealing with the energy value H_0 rather than the period $\overline{T}$ to detect periodic orbits.

5 Applications to celestial mechanics and astrodynamics

The following numerical tests are mainly concerned with the motion of a body with negligible mass (planetoid) in the gravitational field generated by two celestial bodies with finite mass (primaries) rotating around their common center of mass in circular orbits. Such a dynamical system is referred to as the *circular restricted three-body problem* (CRTBP) and its interest goes back to the second quarter of the eighteenth century, in the context of the lunar theory [1]. A renewed interest arose starting from the late 1960s up to present day and is testified by a rich and growing literature on the design and analysis of a variety of orbits connected with the motion of spacecrafts, satellites and asteroids [14, 19, 21, 29, 33].

We here consider the case where the two primaries are the Sun and the Earth+Moon whose masses are denoted m_1 and m_2. Usually the units are normalized and chosen so that the properties of the resulting dynamical system depend on a single parameter μ, defined as the ratio $\frac{m_2}{m_1+m_2}$. In our situation we have $\mu = 3.04036 \cdot 10^{-6}$. To obtain dimensionless coordinates the following normalizing assumptions are introduced:

1. the total mass of the system is $m_1 + m_2 = 1$;
2. the unit of length is the distance between the two primaries, i.e., $R = 1.49589 \cdot 10^8$km;
3. the unit of time is $1/n$, where $n = 1.99099 \cdot 10^{-7}$rad/s is the constant angular velocity of the Sun and Earth/Moon around their center of mass C_M.

Notice that, from the above hypotheses, the gravitational constant is unity, $G = 1$. It is also common to write down the equations of motion of the planetoid in a frame where the primaries are stationary. This is accomplished by introducing a rotating (synodic) orthogonal frame centered at C_M, with the x-y axes lying in the plane of the Sun-Earth/Moon orbit, the x-axis being oriented from the Sun toward the Earth, and the z-axis forming a right-hand frame with the other axes. Thus, the Sun and the Earth are located on the x-axis at the abscissae $-\mu$ and $1-\mu$ respectively.

Let $q(t) = [q_1(t), q_2(t), q_3(t)]^\top$ be the coordinates of the planetoid at time t and set $p(t) = [p_1(t), p_2(t), p_3(t)]^\top \equiv [\dot{q}_1(t) - q_2(t), \dot{q}_2(t) + q_1(t), \dot{q}_3(t)]^\top$ the vector of conjugate momenta. The Hamiltonian function in non-dimensional form associated with the dynamical system governing the motion of the planetoid is

$$H(q, p) = p_1 q_2 - p_2 q_1 + \frac{1}{2} p^\top p - \frac{1-\mu}{r_1} - \frac{\mu}{r_2}, \tag{42}$$

where $r_1 = ((q_1 + \mu)^2 + q_2^2 + q_3^2)^{1/2}$ and $r_2 = ((q_1 - (1-\mu))^2 + q_2^2 + q_3^2)^{1/2}$ are the distances of the planetoid from the Sun and the Earth/Moon respectively.

It is well-known that such a dynamical system admits five equilibrium points referred to as *Lagrangian* or *libration* points: three (L_1, L_2, L_3) are collinear with the primaries and the other two (L_4 and L_5) form an equilateral triangle with them.

Periodic and quasi-periodic orbits around libration points are suited for a number of mission applications. For example, Sun-Earth libration points are commonly used for deep space or Sun activity observations. In the following experiments we are

interested in the dynamics around L_2, which is located beyond the Earth, on the x-axis, at the abscissa 1.010075.

An interesting problem in astrodynamics is the *optimal transfer trajectory*, which consists in finding the optimal control laws that drive a spacecraft from an initial state, say P_1, to a desired final state P_2 in a given time T. Here, the term *optimal* means that the amount of propellant needed to produce the change in orbital elements is minimized.

Since the fuel consumption is proportional to changes in the velocity, an input vector $u(t) = [u_1(t), u_2(t), u_3(t)]^\top$ enters the dynamical system to control the acceleration of the vehicle along the three axes. This is accomplished by considering a new non-autonomous Hamiltonian function

$$\bar{H}(q, p) = H(q, p) + q^\top u,$$

where $H(q, p)$ is as in (42). Our optimal control problem is then formulated as follows:

Minimize the quadratic cost $J = \frac{1}{2}\int_0^T ||u(t)||_2^2 \mathrm{d}t$, *subject to the dynamics induced by* $\bar{H}(q, p)$ *and the boundary conditions corresponding to the states* P_1 *and* P_2.

We assume that the control input is unconstrained and regular. The Pontryagin maximum principle is often used to attack this problem. Setting $y^\top = [q^\top, p^\top]$ (state variables) and $\lambda = [\lambda_1, \ldots, \lambda_6]^\top$ (costate variables), one considers the augmented Hamiltonian function

$$\widetilde{H}(y, \lambda, u) = \frac{1}{2}u^\top u + \lambda^\top J \nabla \bar{H}(q, p).$$

Then, the necessary conditions for optimality are

$$\dot{y} = \frac{\partial \widetilde{H}}{\partial \lambda}, \qquad \dot{\lambda} = -\frac{\partial \widetilde{H}}{\partial y}, \qquad \frac{\partial \widetilde{H}}{\partial u} = 0.$$

The third equation gives $u_i = -\lambda_{(3+i)}$, $i = 1, 2, 3$, so that the resulting system is autonomous and only depends on the state and costate variables. It is defined by the Hamiltonian

$$\begin{aligned} \widehat{H}(y, \lambda) &= \tfrac{1}{2}(\lambda_4^2 + \lambda_5^2 + \lambda_6^2) + \lambda^\top (J \nabla H(q, p) - [0, 0, 0, \lambda_4, \lambda_5, \lambda_6]^\top) \\ &= \lambda^\top J \nabla H(q, p) - \tfrac{1}{2}(\lambda_4^2 + \lambda_5^2 + \lambda_6^2). \end{aligned} \tag{43}$$

We now consider a few applications concerning the above problems. All experiments have been carried out in Matlab (in double precision arithmetic) by using its sparse linear solvers.[7]

[7] More efficient linear solvers will be studied elsewhere.

5.1 Computation of Lyapunov orbits

Lyapunov orbits are periodic orbits surrounding a libration point in the planar CRTBP, where the term *planar* means that the planetoid moves in the same plane as the primaries, namely the x-y plane: $q_3(t) = 0$, $p_3(t) = \dot{q}_3(t) = 0$. We are interested in the computation of Lyapunov orbits emanating from the point L_2, which we here assume as the origin of the axes. Their existence is guaranteed by Lyapunov's center theorem [26], which also states that Lyapunov orbits form a one-parameter family parametrized by the Hamiltonian integral. Thus, it makes sense to search for a Lyapunov orbit by fixing either its period or its energy level. We consider both situations and notice that in the latter case an energy-conserving method is more appropriate since it provides a numerical solution that precisely lies on the required energy set. An analysis of the monodromy matrix associated with Lyapunov orbits shows their instability character, which makes their computation a delicate issue.

We discretize the time interval into $n = 100$ uniform points and use the method HBVM(6, 2) which ensures a practical energy conservation for the problem at hand and the used stepsize (see (10)). As initial condition for the Newton iteration, we consider a periodic orbit very close to the equilibrium point L_2 obtained as the solution of the linearized problem: it is the closed curve labelled as σ_0 in Fig. 1 and corresponds to a period $T = 178$ days. The symmetry of Lyapunov orbits with respect to the y-axis suggests to use $q_2 = 0$ as anchor equation for the solution at time $t = 0$ (see (40)).

The curve σ_1 denotes the Lyapunov orbit with period $T = 200$ days and has been obtained by considering periodic boundary conditions and a fixed stepsize $h = \frac{T}{n}$, as discussed at the end of Section 4. The energy level associated with this orbit is $H_2 \simeq -1.5002604$.

Starting from σ_1, we attempt to find the Lyapunov orbit corresponding to the energy level $H_3 = -1.5001$ and thus we solve the iteration described at (41). We obtain the orbit labelled as σ_2 in Fig. 1: its period is $T_3 \simeq 251.34$ days. Figure 1 also displays the energy errors related to the orbits σ_1 and σ_2, and confirms the energy-preservation properties of HBVM(6, 2) for this specific set of data.

The search of σ_2 via its period T_3 rather than its energy level H_3 starting from σ_1 would not provide the desired result: whatever method in the family HBVM(k, 2) we choose, the iteration process converges to a different periodic orbit σ_3 that embraces the Lagrangian points L_1 and L_2 other than the Earth. This orbit has period T_3 but its energy is $H_3 \simeq -1.500177$. To retrieve the correct Lyapunov orbit we need to compute an intermediate curve, such as σ_4, that has been obtained by fixing the period $T_4 = 220$ days.

5.2 The Hill three-body problem

The Hill problem is a special, simplified case of the planar CRTBP. It studies the motion of the planetoid in a neighborhood of the Earth, which is conveniently taken as the new origin of the synodic frame via the change of coordinates $q_1 \to q_1 + (1-\mu)$, $q_2 \to q_2$. The assumption on the location of the planetoid permits a simplification of the equations describing its dynamics. Essentially, one discards the terms of order

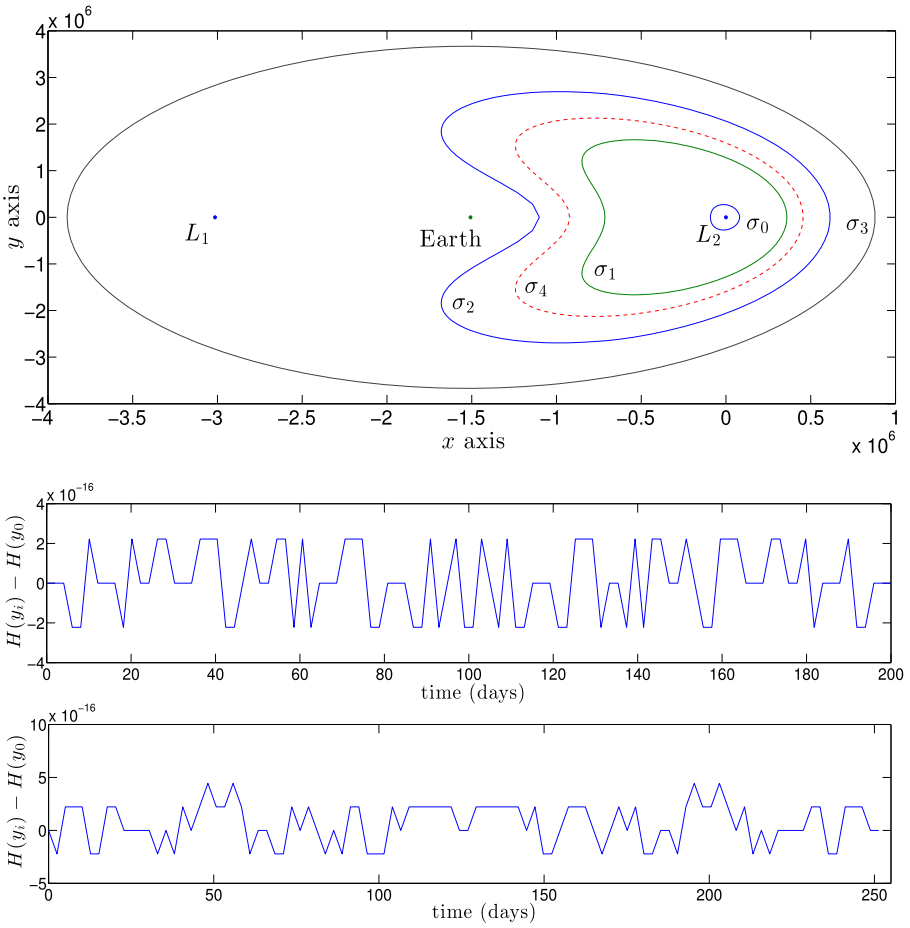

Fig. 1 *Upper picture*: some Lyapunov orbits surrounding the libration point L_2. Their computation may be carried out by passing as input information either their period or their energy level. *Lower pictures*: error in the Hamiltonian function evaluated along the numerical solutions corresponding to the orbit σ_1 (*intermediate plot*) and σ_2 (*bottom plot*)

at least three in q_1 and q_2 in the Taylor expansion of the potential around $(0, 0)$, and performs an additional change of variables to simplify the final shape of the equations, making them independent of the parameter μ (see, for example, [4] for details). The Hamiltonian function arising from these transformations reads

$$H(q_1, q_2, p_1, p_2) = p_1 q_2 - p_2 q_1 + \frac{1}{2}(p_1^2 + p_2^2) - \frac{1}{(q_1^2 + q_2^2)^{1/2}} + \frac{1}{2}q_2^2 - q_1^2. \quad (44)$$

This reduced system admits only two equilibrium points located on the x-axis on both sides of the Earth: $L_1 = \left(-(1/3)^{1/3}, 0\right)$ and $L_2 = \left((1/3)^{1/3}, 0\right)$.

We consider an optimal transfer problem, taken from [16], consisting in transferring a spacecraft from the point $L_2 = ((1/3)^{1/3}, 0)$ to the point $P = ((1/3)^{1/3} +$

0.005, 0.0044). In both points the velocity is assumed null and the transfer time is increased as $t_f = 0.1, 2.1, 4.1, 6.1, 8.1$. The number of points in the numerical approximation is $n = 50$, thus the stepsize is $h = \frac{t_f}{n}$. Due to the fact that the dynamics takes place near an equilibrium point, we choose the HBVM(4, 2) method as integrator, since two silent stages are enough to guarantee a practical energy conservation. The top picture in Fig. 2 shows the five trajectories of the spacecraft corresponding to the selected transfer times. As t_f is increased, the spacecraft circles around the point L_2, in a spiral-shaped orbit, before approaching the final point P. The intermediate plot of Fig. 2 reports the relative error in the Hamiltonian function (44) evaluated along the numerical solution $\{y_i\}$ corresponding to $t_f = 8.1$. We notice that it is bounded by 10^{-10} and cannot be further reduced even if we increase the number of silent stages. This is an effect of the use of finite precision arithmetic

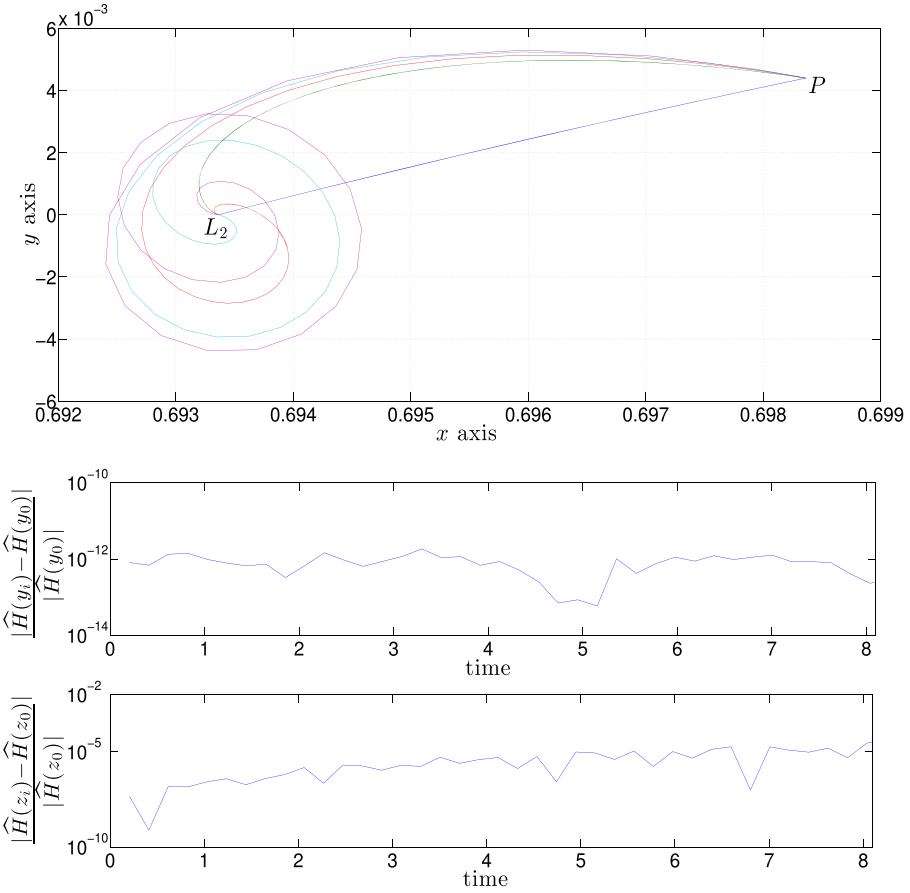

Fig. 2 *Upper picture*: orbits of a spacecraft driven from the libration point L_2 to a close point P for several transfer times. *Lower pictures*: relative error in the Hamiltonian function (43) evaluated along the numerical solutions obtained by the HBVM(4, 2) (*intermediate plot*) and the Gauss method of order 4 (*bottom plot*). Both solutions correspond to $t_f = 8.1$

and the fact that the order of the Hamiltonian along the orbit is 10^{-6}. For comparison purposes, in the bottom plot of Fig. 2, we have also included the corresponding error produced by the 4-th order Gauss method (i.e., HBVM(2,2)).

5.3 Computation of halo orbits

Halo orbits are out-of-plane periodic orbits which trace a halo around the Earth. We are interested in reproducing halo orbits around the point L_2. They consist of two one-parameter families of periodic orbits referred to as halo orbits of class I and II (see [30]), where the parameter may be either the energy or the period.

We have implemented the HBVM$(6, 2)$ formula and adapted the algorithm in order to compute periodic solutions in the two different situations where we are given either the period $T \equiv t_f - t_0$ of the orbit or its energy level H_0. In the latter case, according to what was said in Section 4, the stepsize of integration h is regarded as an extra unknown and the scalar equation $H(q_0, p_0) = H_0$ is added to the set of boundary conditions.

In both cases, an elliptic curve lying on a plane orthogonal to the x-axis and passing through L_2 has been chosen as initial guess for the Newton iteration. More specifically, the starting (and ending) point P_0 of this curve has been set at the upper end of the vertical axis of the ellipse (see Fig. 3), and its sense of revolution about L_2 is clockwise as viewed into the negative direction of the x-axis. This initial condition will allow us to detect halo orbits of class I. Halo orbits in this family are symmetric with respect to the x-y plane. Consequently, we have introduced the anchor equation $q_2 = 0$ for the solution at time $t = 0$. The number of points in the numerical approximation is $n = 100$.

The left picture of Fig. 3 displays the initial guess (dashed line) together with two halo orbits (solid lines). The inner one is the halo orbit corresponding to a period $T_1 =$

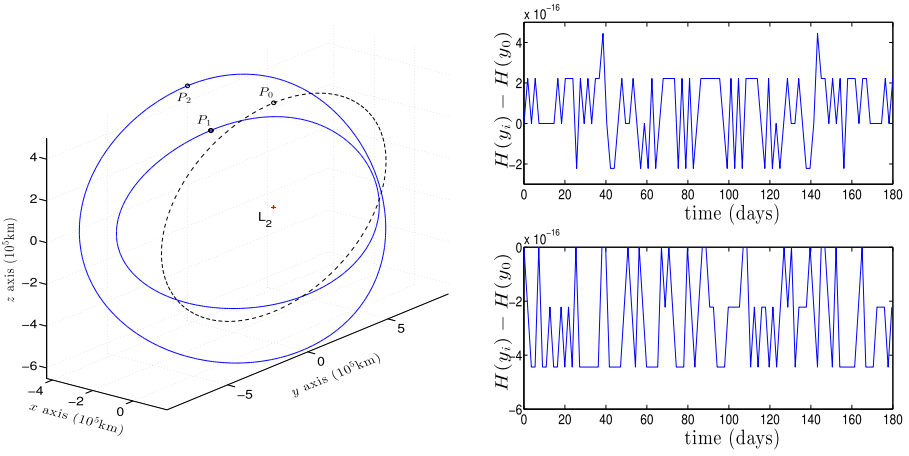

Fig. 3 *Left picture*: two halo orbits around the libration point L_2 (*solid lines*) and the initial guess for the Newton iteration scheme associated to the method (*dashed line*). *Right picture*: the Hamiltonian function (42) is precisely conserved along the numerical solutions

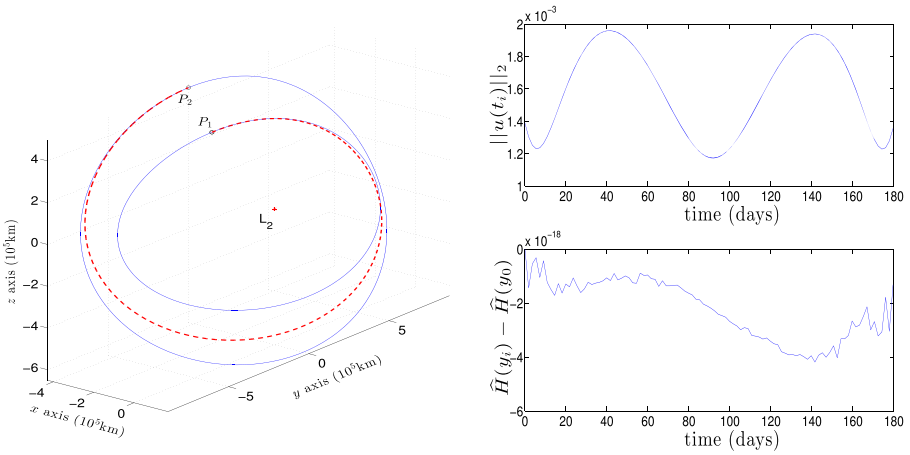

Fig. 4 *Left picture*: optimal transfer orbit between two halo orbits (*dashed line*). *Right picture*: norm of the optimal control variable $u(t)$ (*upper plot*) and error in the Hamiltonian function (43) (*lower plot*)

180 days. The energy level of this first numerical approximation is $H_1 \approx -1.500394$. Conversely, the outer halo orbit has been computed on the basis of its energy level, which has been set to $H_2 = -1.50036$. Notice that in the non-dimensional system $H_2 \approx H_1(1 + 2 \cdot 10^{-5})$ while the actual distance of the topmost points of the two orbits is $\overline{P_1 P_2} = 2 \cdot 10^5$km. The period corresponding to the energy level H_2 is $T_2 = 179.19$ days. The right pictures of Fig. 3 show that the energy error is close to the machine precision in both cases.

We also consider the optimal transfer trajectory problem consisting in transferring a spacecraft from the inner to the outer halo orbit and, specifically, from the point P_1 to the point P_2. In Fig. 4 we show the optimal control orbit joining the points P_1 and P_2 in a time $T = (T_1 + T_2)/2$ (left picture, dashed line) together with the norm of the optimal control variable $u(t)$ and the error $\widehat{H}(y_n) - \widehat{H}(y_0)$ in the Hamiltonian (43) (right picture).

6 Conclusions

In this paper, we have extended the use of HBVMs to the solution of Hamiltonian Boundary Value Problems. HBVMs form a subclass of Runge–Kutta methods, characterized by a rank-deficient coefficient matrix, that provide a numerical solution along which the Hamiltonian function is precisely conserved. Their implementation has been adapted in order to handle different kinds of boundary conditions. In particular, separated and periodic boundary conditions arise in several problems of celestial mechanics and astrodynamics, such as the periodic orbit detection and the optimal spacecraft transfer trajectory. A few numerical tests in this direction have shown the good potentialities of the methods.

Acknowledgments We thank the anonymous reviewers for the careful reading of our manuscript and their many insightful comments and suggestions.

References

1. Alexander, D.S., Iavernaro, F., Rosa, A.: Early days in complex dynamics. A history of complex dynamics in one variable during 1906–1942. History of Mathematics, vol. 38. American Mathematical Society, Providence (2012)
2. Amodio, P., Cash, J.R., Fairweather, G., Gladwell, I., Kraut, G.L., Roussos, G., Paprzycki, M., Wright, R.W.: Almost block diagonal linear systems: sequential and parallel solution techniques, and applications. Numer. Linear Algebra Appl. **7**, 275–317 (2000)
3. Amodio, P., Romanazzi, G.: Algorithm 859: BABDCR–a Fortran 90 package for the solution of Bordered ABD linear systems. ACM Trans. Math. Softw. **32**, 597–608 (2006)
4. Arnold, V.I., Kozlov, V.V., Neishtadt, A.I.: Mathematical aspects of classical and celestial mechanics. Encyclopaedia Math. Sci., 3rd edn., vol. 3. Springer-Verlag, Berlin (2006)
5. Ascher, U.M., Mattheij, R.M.M., Russell, R.D.: Numerical solution of boundary value problems for ordinary differential equations. Classics in Applied Mathematics, vol. 13. Society for Industrial and Applied Mathematics (SIAM), Philadelphia (1995)
6. Battin, R.H.: An introduction to the mathematics and methods of astrodynamics. Revised edition. American Institute of Aeronautics and Astronautics (AIAA), Reston (1999)
7. Brugnano, L., Iavernaro, F., Trigiante, D.: Isospectral Property of Hamiltonian Boundary Value Methods (HBVMs) and their blended implementation. arXiv:1002.1387[math.NA] (2010)
8. Brugnano, L., Iavernaro, F., Trigiante, D.: A note on the efficient implementation of Hamiltonian BVMs. J. Comput. Appl. Math. **236**, 375–383 (2011)
9. Brugnano, L., Iavernaro, F., Trigiante, D.: Hamiltonian Boundary Value Methods (energy preserving discrete line methods). J. Numer. Anal. Ind. Appl. Math. **5**(1–2), 17–37 (2010)
10. Brugnano, L., Iavernaro, F., Trigiante, D.: The lack of continuity and the role of infinite and infinitesimal in numerical methods for ODEs: the case of symplecticity. Appl. Math. Comput. **218**(16), 8053–8063 (2012)
11. Brugnano, L., Iavernaro, F., Trigiante, D.: A simple framework for the derivation and analysis of effective one-step methods for ODEs. Appl. Math. Comput. **218**(17), 8475–8485 (2012)
12. Deuflhard, P.: Computation of periodic solutions of nonlinear ODE's. BIT **24**, 456–466 (1984)
13. Deuflhard, P.: Newton methods for nonlinear problems. Affine invariance and adaptive algorithms. Springer Series in Computational Mathematics, vol. 35. Springer, Heidelberg (2011)
14. Farquhar, R.W.: Halo-orbit and lunar-swingby missions of the 1990s. Acta Astronautica **24**, 227–234 (1991)
15. Fiedler, B.: Global bifurcation of periodic solutions with symmetry. Lecture Notes in Mathematics. Springer Verlag, Berlin (1988)
16. Guibout, V.M., Scheeres, D.J.: Solving two-point boundary value problems using the Hamilton-Jacobi theory. Proceedings of the 2nd WSEAS Int. Conference on Applied and Theoretical Mechanics, Venice, Italy (2006)
17. Gustafson, E.D., Scheeres, D.J.: Dynamically Relevant Local Coordinates for Halo Orbits. AIAA/AAS Astrodynamics Specialist Conference and Exhibit, Honolulu (2008)
18. Hairer, E., Lubich, C., Wanner, G.: Geometric numerical integration. Structure-preserving algorithms for ordinary differential equations, 2nd edn. Springer, Berlin (2006)
19. Howell, K.C.: Three-dimensional, periodic, "halo" orbits. Celestial Mech. **32**(1), 53–71 (1984)
20. Iavernaro, F., Trigiante, D.: High-order symmetric schemes for the energy conservation of polynomial Hamiltonian problems. J. Numer. Anal. Ind. Appl. Math. **4**(1-2), 87–101 (2009)
21. Jorba, A., Masdemont, J.: Dynamics in the center manifold of the collinear points of the restricted three body problem. Phys. D **132**, 189–213 (1999)
22. Keller, H.B.: Numerical methods for two-point boundary value problems. Ginn-Blaisdell, Waltham (1968)
23. Koon, W.S., Lo, M.W., Marsden, J.E., Ross, S.D.: Dynamical systems, the three-body problem and space mission design. Marsden Books. Available at URL: http://www.shaneross.com/books/space (2011)

24. Lakshmikantham, V., Trigiante, D.: Theory of difference equations: numerical methods and applications. Monographs and Textbooks in Pure and Applied Mathematics, vol. 251, 2nd edn. Marcel Dekker, Inc., New York (2002)
25. Leimkuhler, B., Reich, S.: Simulating Hamiltonian dynamics. Cambridge University Press, Cambridge (2004)
26. Meyer, K.R., Hall, G.R., Offin, D.: Introduction to Hamiltonian dynamical systems and the N-body problem. Applied Mathematical Sciences, vol. 90, 2nd edn. Springer, New York (2009)
27. Muñoz-Almaraz, F.J., Freire, E., Galán, J., Doedel, E., Vanderbauwhede, A.: Continuation of periodic orbits in conservative and Hamiltonian systems. Phys. D **181**(1-2), 1–38 (2003)
28. Nayfeh, A.H., Balachandran, B.: Applied nonlinear dynamics; Analytical, computational and experimental methods. Wiley-International, Chichester (1995)
29. Peng, H.J., Gao, Q., Wu, Z.G., Zhong, W.X.: Symplectic adaptive algorithm for solving nonlinear two-point boundary value problems in Astrodynamics. Celestial Mech. Dynam. Astronom. **110**, 319–342 (2011)
30. Richardson, D.L.: Analytical construction of periodic orbits about the collinear points. Celestial Mech. **22**, 241–253 (1980)
31. Sanz-Serna, J.M., Calvo, M.P.: Numerical Hamiltonian problems, AMMC 7. Chapman & Hall (1994)
32. Sepulchre, J.-A., Mac Kay, R.S.: Localized oscillations in conservative or dissipative networks of weakly coupled autonomous oscillators. Nonlinearity **10**(3), 679–713 (1997)
33. Serban, R., Koon, W., Wang, S., Lo, M.W., Marsden, J.E., Petzold, L.R., Ross, S.D., Wilson, R.S.: Halo orbit mission correction maneuvers using optimal control. Automatica J. IFAC **38**(4), 571–583 (2002)
34. Wulff, C., Schebesch, A.: Numerical continuation of hamiltonian relative periodic orbits. J. Nonlinear Sci. **18**, 343–390 (2008)